European Journal of Pharmacology 725 (2014) 1–9

Contents lists available at ScienceDirect

European Journal of Pharmacology

journal homepage: www.elsevier.com/locate/ejphar

Molecular and cellular pharmacology

Involvement of transient receptor potential melastatin-8 (TRPM8) in menthol-induced calcium entry, reactive oxygen species production and cell death in rheumatoid arthritis rat synovial fibroblasts

Shuyan Zhu [1], Yuxiang Wang [1], Leiting Pan *, Shuang Yang, Yonglin Sun, Xinyu Wang, Fen Hu **

School of Physics and TEDA Applied Physics Institute, Key Laboratory of Bioactive Materials of Education Ministry, Nankai University, Tianjin, China

ARTICLE INFO

Article history:
Received 27 June 2013
Received in revised form
20 December 2013
Accepted 7 January 2014
Available online 15 January 2014

Keywords:
Menthol
TRPM8
Calcium
Synoviocytes
Apoptosis
Reactive oxygen species

ABSTRACT

Rheumatoid arthritis is most prominently characterized by synoviocyte hyperplasia which therefore serves as an important target for clinical therapy. In the present study, it was observed that menthol, the specific agonist of transient receptor potential melastatin subtype 8 (TRPM8), could induce sustained increases of cytosolic calcium concentration ($[Ca^{2+}]_c$) in synoviocytes isolated from collagen-induced arthritis rats in dose-dependent manner, which was evidently blocked by applying an extracellular Ca^{2+}-free buffer. Menthol-induced $[Ca^{2+}]_c$ increase was also significantly inhibited by potent TRPM8 antagonist capsazepine (CZP), indicating that this $[Ca^{2+}]_c$ elevation was mostly attributed to TRPM8-mediated Ca^{2+} entry. Besides, RT-PCR indeed demonstrated presence of TRPM8 in the synoviocytes. Meanwhile, it was found that menthol evoked production of intracellular reactive oxygen species, which could be abolished by Ca^{2+} free solutions or CZP. Further experiments showed that menthol reduced the cell numbers and survival of synoviocytes. This reduction was associated with apoptosis as suggested by mitochondrial membrane depolarization, nuclear condensation and a caspase 3/7 apoptotic assay. Menthol-induced death and apoptosis of synoviocytes both were obviously inhibited by CZP, intracellular calcium chelator BAPTA-AM, and reactive oxygen species inhibitor diphenylene iodonium, respectively. Taken together, our data indicated that menthol resulted in synoviocyte death associated with apoptosis via calcium entry and reactive oxygen species production depending on TRPM8 activation.

1. Introduction

Rheumatoid arthritis (RA) is an autoimmune and chronic disease characterized by inflammatory synovitis, leading eventually to cartilage and bone destruction, affecting over 50 millions people in the world (Firestein, 2003; McInnes and Schett, 2007). The etiology of this systemic inflammatory disorder is complex, and uncontrolled synoviocyte hyperplasia is an important feature in the genesis and development of RA (Bartok and Firestein, 2010). Relevant drug investigation and clinical application have been concentrated on the research of specific compounds which could lead to cell death or premature apoptosis in the affected RA tissue (Macpherson et al., 2006; Sherkheli et al., 2008).

Menthol ((1R, 2S, 5R)-2-isopropyl-5-methyl cyclohexanol) is a cyclic terpene alcohol produced by the peppermint herb, *Mentha piperita* (Al-Bayati, 2009; Patel et al., 2007). It elicits a pleasant cool sensation, and is widely used in food, cosmetics, and pharmaceutical products for treatment of asthma, headache, vertigo, and pain relieving (Eccles, 1994). As a natural compound with complex sensory effects, menthol exhibits multiple biological activities including anti-inflammation (Macpherson et al., 2006), antivirus (Al-Bayati, 2009), and antitumor (Kim et al., 2009; Wondergem and Bartley, 2009). Specially, it has been proposed that menthol acts on some membrane ion channels represented by transient receptor potential (TRP) channels (Sherkheli et al., 2010).

Transient receptor potential melastatin (TRPM) channels, the largest subfamily of TRP class, perform diverse functions ranging from detection of cold, osmolarity, redox state and cell proliferation or death (Clapham, 2003; Clapham et al., 2001; Zholos, 2010). TRPM8, a submember of TRPM, is predominantly expressed in sensory neurons, dorsal root ganglia, as well as prostate and other cancer cells (Dhaka et al., 2006; Journigan and Zaveri, 2013; McKemy et al., 2002; Yudin and Rohacs, 2012). It plays important roles in various pathological processes including pain sensation (Caspani et al., 2009; Levine and Alessandri-Haber, 2007; Proudfoot et al., 2006), inflammatory hyperalgesia (Sherkheli et al., 2010) and tumor migration (Yamamura et al., 2008).

* Corresponding author. Tel.: +86 22 66229610.
** Corresponding author. Tel: +86 22 23508390.
E-mail addresses: plt@nankai.edu.cn (L. Pan), hufen@nankai.edu.cn (F. Hu).
[1] These authors contributed equally.

0014-2999/$ - see front matter © 2014 Elsevier B.V. All rights reserved.
http://dx.doi.org/10.1016/j.ejphar.2014.01.001

Accordingly, TRPM8 responds to cooling stimuli induced by cold temperatures or chemical agonists such as menthol and icilin (Zakharian et al., 2010). Upon the activation of TRPM8, extracellular calcium can enter into the cell via this Ca^{2+}-permeable channel, resulting in an increase in cytosolic Ca^{2+} concentration ($[Ca^{2+}]_c$) (Peier et al., 2002; Thebault et al., 2005). This $[Ca^{2+}]_c$ increase eventually led to reduction of cellular viability in human melanoma (Yamamura et al., 2008), apoptosis in tumor cells like the prostate cancer-derived epithelial cell line (Park et al., 2009) and cell migration in human glioblastoma (Wondergem and Bartley, 2009). Studies also showed that TRPM8 mediated histamine release in mast cells (Cho et al., 2010), and analgesia in dorsal root ganglia neurons (Proudfoot et al., 2006).

Recently, the existence and expression of various types of TRP channels including TRPM8, TRPV1, TRPV4 have been detected in synovial fibroblasts from RA patients (Journigan and Zaveri, 2013; Biro et al., 2007; Kochukov et al., 2006). Our previous studies showed that TRPV1 and TRPV4 were implicated in the pathology of RA (Hu et al., 2008; Sun et al., 2008). However, the functions of other TRP channels in RA and underlying intracellular signaling remained largely unknown. In the present study, we examined the effects of menthol on $[Ca^{2+}]_c$, intracellular reactive oxygen species, mitochondrial membrane potential, caspase 3/7 activities, and cell survival in the arthritic rat synoviocytes, and investigated the roles of TRPM8 in these processes.

2. Materials and methods

2.1. Animals and reagents

Male Wistar rats weighing 200 ± 50 g were obtained from Institute of Health and Environmental Medicine, Academy of Military Medical Sciences (Tianjin, China). Dulbecco's modified Eagle's medium (DMEM) and fetal bovine serum (FBS) were purchased from Gibco (Gaithersburg, MD, USA) and HyClone (Logan, UT, USA) respectively. Fura 2-AM was from Biotium (Hayward, CA, USA). RNAprep pure Cell/Bacteria Kit was from TIANGEN BIOTECH (Beijing, China). Reverse Transcription System, GoTaq PCR Core system and Caspase-Glo assay kit were from Promega (Madison, WI, USA). The rest of the reagents, including menthol, capsazepine (CZP), diphenylene iodonium (DPI), dihydroethidium (DHE), 3-(4,5-dimethylthiazol-2-yl)-3,5-diphenyltetrazolium bromide (MTT), trypsin, Hoechst 33342, Rhodamine 123, EGTA, BAPTA-AM and collagenase II were purchased from Sigma-Aldrich (St. Louis, MO, USA).

2.2. Isolation and culture of synovial fibroblasts

The collagen-induced arthritis rat models were established as reported (Shou et al., 2006), and the synovial fibroblasts were isolated and cultured as described (Hinoi et al., 2005). Briefly, rats with arthritis were sacrificed and their hind limbs were excised. Synovial membranes of the knee joints were carefully separated and minced in D-Hank's solution (NaCl 150 mM, KCl 5.4 mM, Na_2HPO_4 3 mM, KH_2PO_4 2 mM, Glucose 10 mM, pH = 7.4). Then, the synovial tissue was digested in 0.2% collagenase for 3 h at 37 °C in serum-free DMEM. After that, the cell suspension was centrifuged at 300*g* for 10 min and the isolated synovial cells were cultured in DMEM supplemented with 10% FBS in a humidified CO_2 incubator with 5% CO_2 at 37 °C. The cultured cells must be subjected to a minimum of 6 passages to obtain a pure culture for experiments as previously described.

2.3. Measurement of cytosolic Ca^{2+} concentrations ($[Ca^{2+}]_c$)

Synoviocytes were incubated in Hanks' balanced salt solution (HBSS) (NaCl 150 mM, KCl 5.4 mM, $CaCl_2$ 2 mM, $MgCl_2$ 1 mM, Glucose 10 mM and HEPES 10 mM, pH = 7.4) with 5 μM Fura 2-AM for 1 h at room temperature. After being washed gently and extensively with HBSS, cells were bathed in fresh HBSS. $[Ca^{2+}]_c$ was measured in a calcium imaging system built on an inverted fluorescence microscope (Olympus IX51). The ratiometric fluorescent Ca^{2+} indicator dye Fura 2 was alternately excited at 340 nm and 380 nm with a Lambda 10-2 optical filter changer (Sutter Instrument, USA). Fluorescence images (filtered at 515 nm ± 25 nm) were captured by a CCD camera (CoolSNAP fx-M, Roper Scientific Inc.) and quantitated with MetaFluor 5.0 (Universal Imaging Corporation, USA). All experiments were performed at room temperature in dark and $[Ca^{2+}]_c$ was represented by the ratio of fluorescence intensity at 340 nm/fluorescence intensity at 380 nm (F340/F380). At least three independent experiments were done for each condition and 5–10 individual cells were selected randomly in each experiment. One curve of calcium changes was plotted as the representation of other similar traces. Calcium-free HBSS was prepared by substituting $MgCl_2$ for $CaCl_2$ at the same concentration, with 2 mM EGTA added.

2.4. RNA isolation and RT-PCR

Total RNA from synoviocytes was isolated using RNAprep pure Cell/Bacteria Kit. Then, the RNA (1 μg) was subjected to reverse transcription using a reverse transcription system (Promega, USA) in a total volume of 20 μl reaction that contained $MgCl_2$ (5 mM), dNTP mixture (1 mM), oligo$(dT)_{15}$ primer (0.5 μg), RNase inhibitor (0.5 μl), reverse transcription 10 × buffer (2 μl), and AMV reverse transcriptase (15 U). The reaction mixtures were incubated at 42 °C for 30 min, 99 °C for 5 min to inactivate the enzyme, and then chilled on ice for 5 min. Subsequently, the product of RT reaction (1 μl) was amplified using a GoTaq PCR Core system (Promega, USA) in a total volume of 50 μl PCR buffer containing Green Master Mix (25 μl), sense primer (100 pM) and antisense primer (100 pM). The reaction mixtures were preheated to 95 °C for 2 min followed by 40 thermal cycles in a PCR machine (MJMini™, BIO-RAD, USA). For each cycle, denaturation was at 95 °C for 30 s, annealing at 61 °C for 30 s, and extension at 72 °C for 1 min. PCR primers were as follows: TRPM8 sense: 5′-ATCCCCATCGTGTGTTTTGC-3′, antisense: 5′-GAGGCGGACAAACTTGGGC-3′, encompassing 534 bp of the published rat TRPM8 sequence; GAPDH (glyceraldehyde-3-phosphate dehydrogenase, as positive control) sense: 5′-GTGGAGTCTACTGGCGTCTT-3′, antisense: 5′-CCAGGATGCCCTTTAGTG-3′, encompassing 537 bp.

2.5. Detection of intracellular reactive oxygen species

DHE, a reduced form of ethidium bromide, was used to detect and measure intracellular production of reactive oxygen species. After stimulation with indicated reagents for 1 h, synoviocytes were incubated in HBSS with 5 μM DHE for 30 min at 37 °C. The cells were then imaged after being rinsed twice. The excitation wavelength of DHE is at 488 nm and fluorescent images (after a 610 nm band-pass filter) were captured by CCD. MetaFluor was used to analyze the fluorescence intensity, which is indicative of the reactive oxygen species level.

2.6. Proliferation assay

The cells were plated in 24-well plates (1 ml; 1×10^5 cells/ml) at 37 °C in DMEM with 5% FBS, then trypsinized and counted three

times with a hemocytometer after treatment for the indicated time.

2.7. Cell viability assay

Synoviocyte viability was assessed with MTT. Cell suspension (200 μl; 1×10^5 cells/ml) was seeded into a 96-well plate and incubated with or without test reagents for 48 h at 37 °C in DMEM with 5% FBS. Four hours before the end of such treatment, 10 μl MTT solution (10 mg/ml in HBSS) was added, with reactions stopped by removal of medium and addition of 100 μl of lysis buffer (50% DMSO, 50% ethanol). The absorbance at 570 nm (A_{570}) for each well was determined by an ELISA reader (Bio-Rad Imark Microplate Reader) to determine cell viability. The cell viability of control group (untreated cells) was regarded as 100%. The cell viability of other groups was normalized to control and calculated as $(A_{570,\ test}/A_{570,\ control}) \times 100\%$.

2.8. Detection of mitochondrial membrane potential

Rhodamine 123 was used to assess mitochondrial membrane potential. Cell suspension (2 ml; 1×10^4 cells/ml) was seeded into a 6-well plate and incubated in HBSS with Rhodamine 123 (10 μg/ml) for 15 min at room temperature after treatment. The Rhodamine 123-loaded cells were washed and imaged with an inverted fluorescence microscope. The excitation wavelength and emission wavelength were 488 nm and 510 nm respectively. A decrease in Rhodamine 123 fluorescence intensity represents mitochondrial membrane depolarization.

2.9. Assessment of apoptotic cells

Hoechst 33342 was used to observe the morphology of cell nuclei. Cell suspension (2 ml; 1×10^4 cells/ml) was seeded into a 6-well plate, treated with or without test agents for 48 h, and then stained with Hoechst 33342 (10 μg/ml) for 15 min at room temperature after treatment. The stained cells were subsequently washed and imaged with excitation wavelength and emission wavelength at 340 nm and 510 nm respectively.

2.10. Caspase assay

Caspase 3/7 activities in synoviocytes were measured for the detection of apoptotic events, using a Caspase-Glo assay kit. Briefly, the luminogenic substrate containing the tetrapeptide sequence DEVD is cleaved by caspase 3/7. After caspase cleavage, a luciferase substrate is released, resulting in the luciferase reaction and the production of luminescent signal. Cell suspension (200 μl; 1×10^5 cells/ml) was seeded into a 96-well plate and incubated with or without test reagents for 48 h at 37 °C in DMEM with 5% FBS. After that, an equal volume of reagents was added to each well, and then incubated at room temperature for 2 h. Finally, the luminescence of each sample was measured in a luminometer (GloMax Multi Jr Detection System, Promega, USA). These data from each group were proportional to the amount of caspase activity and were assigned as the relative fluorescence unit (RFU).

2.11. Statistical analysis

All data are presented as mean ± standard deviation (S.D.). The statistical comparison between two groups was carried out using Student's *t*-test (Origin 8.0), and the analysis for multiple groups was using Dunnett's test (SPSS 18.0, one-way ANOVA). $P < 0.05$ was considered to be statistically significant. The values of half maximal effective concentration (EC_{50}) were calculated according to the dose-response curve fitting with the Boltzmann equation

$$y = \frac{A_1 - A_2}{1 + \exp((x - EC_{50})/dx)} + A_2,$$

in which y is the increase in F340/F380 ratio, A_1 is the asymptotic maximum, A_2 is the asymptotic minimum, x is concentrations of menthol and dx is the time constant.

3. Results

3.1. Menthol-triggered $[Ca^{2+}]_c$ increase in synoviocytes was through the activation of TRPM8

The effects of menthol on $[Ca^{2+}]_c$ were measured by calcium imaging system. A rise in F340/F380 ratio indicated an increase of $[Ca^{2+}]_c$. Different concentrations of menthol (20, 100, 200, 500, 1000 μM) all evoked a rapid increase of $[Ca^{2+}]_c$ followed by a sustained high $[Ca^{2+}]_c$ plateau. The amplitude of $[Ca^{2+}]_c$ increase was dependent on the doses of menthol (Fig. 1A). We measured the peak values of $[Ca^{2+}]_c$ increase and plotted against the concentration of menthol (Fig. 1B). The half maximal effective concentration (EC_{50}) of menthol-triggered $[Ca^{2+}]_c$ increase was 250 ± 40 μM, which was calculated according to the dose-dependent curve fitting by Boltzmann equation. Removal of extracellular calcium significantly decreased the rapid $[Ca^{2+}]_c$ increase elicited by menthol (500 μM), and almost eliminated the sustained $[Ca^{2+}]_c$ plateau (Fig. 1C). This data revealed that the sustained increase of $[Ca^{2+}]_c$ was chiefly attributed to extracellular Ca^{2+} influx. Similar responses were observed when the cells were pretreated with TRPM8 antagonist capsazepine (CZP, 5 μM) for 15 min (Fig. 1C), indicating that TRPM8 played key roles in menthol-evoked $[Ca^{2+}]_c$ increase. The statistical analysis of the values of $[Ca^{2+}]_c$ peak and sustained $[Ca^{2+}]_c$ plateau were presented in Fig. 1D from experiments shown in Fig. 1C. Taken together, these results indicated that TRPM8-mediated Ca^{2+} entry was responsible for menthol-induced $[Ca^{2+}]_c$ increase in synoviocytes.

3.2. TRPM8 mRNA expression was detected in the arthritic rat synoviocytes

We used RT-PCR to ascertain the presence of TRPM8 in primary synoviocytes from collagen-induced arthritis rats. The total RNA from synoviocytes was reverse-transcribed and subjected to PCR amplification using the previously cloned specific primers for rat TRPM8 mRNA. As shown in Fig. 2, electrophoresis of PCR products from synoviocytes had the expected intensity band at size of 534 bp, corresponding to TRPM8 sequence. GADPH was used as a positive control with a 537 bp band. This result suggested the expression of TRPM8 at mRNA level in rat synoviocytes.

3.3. Menthol-evoked reactive oxygen species production in synoviocytes was mediated by TRPM8 activation-dependent calcium entry

To investigate signals downstream of $[Ca^{2+}]_c$ elevation after TRPM8 activation, intracellular reactive oxygen species was measured in synoviocytes. Menthol at the concentrations of 100, 500 and 1000 μM evoked marked reactive oxygen species generation after stimulation for 1 h (Fig. 3A*a–d*). In Ca^{2+} free solution or pretreating the cells with CZP (5 μM) for 15 min, the generation of reactive oxygen species induced by menthol (500 μM) was inhibited significantly (Fig. 3A*e*, *f*). The statistical analysis of reactive oxygen species production was presented in Fig. 3B from experiments shown in Fig. 3A. These results indicated that reactive

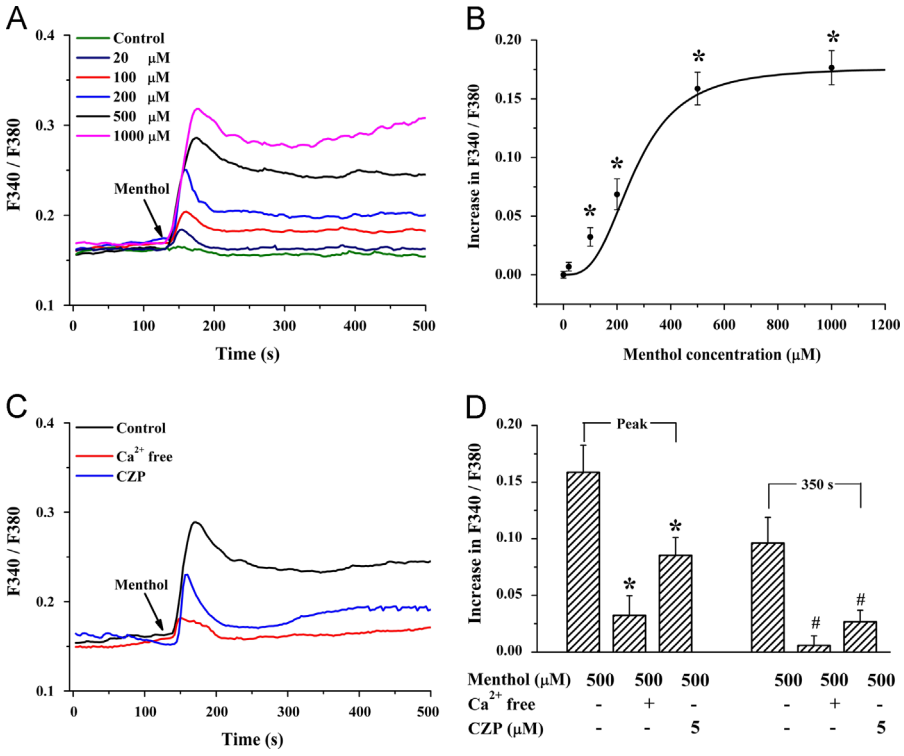

Fig. 1. Menthol induced a sustained increase in $[Ca^{2+}]_c$ in synoviocytes through the activation of TRPM8. (A) Representative $[Ca^{2+}]_c$ traces for stimulating synoviocytes with different concentrations of menthol (20, 100, 200, 500, 1000 μM). (B) The statistic peak values of increase in F340/F380 ratio were plotted against the dose of menthol ($n=15$ for each case), *showed $P<0.05$ comparing with control group. The smooth curve (dose-dependent curve) represented the fitting to the equation.$y=\frac{A_1-A_2}{1+\exp((x-EC_{50})/dx)}+A_2$. (C) Representative $[Ca^{2+}]_c$ traces for stimulating synoviocytes with menthol (500 μM) in Ca^{2+} free solution or after pretreatment with CZP (5 μM) for 15 min. (D) Summary of the peak values and the changes in F340/F380 ratio at 350 s after the application of menthol from experiments shown in C ($n=15$ for each case). * (statistical analysis for peak values) and # (statistical analysis for changes in F340/F380 ratio at 350 s) showed $P<0.05$ comparing with menthol 500 μM group respectively.

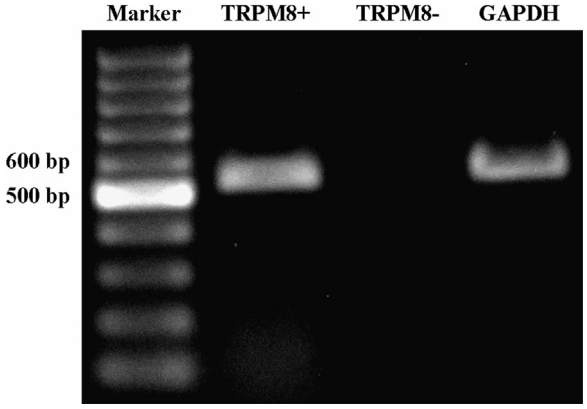

Fig. 2. TRPM8 mRNA was detected in rat synoviocytes by RT-PCR. The four lanes in the gel were as follows: Marker (with a list of standardized DNA sequences from 100 bp to 1000 bp); TRPM8+ (experimental group with primers directed towards the TRPM8 mRNA); TRPM8− (negative control group with nuclease-free water instead of DNA template); GAPDH (positive control group with primers directed towards the GAPDH mRNA).

oxygen species production evoked by menthol was dependent on calcium entry mediated by the activation of TRPM8.

3.4. Menthol-induced decrease of synoviocyte survival was relied on TRPM8 activation

To investigate the proliferation capacity of synoviocytes in response to menthol, we detected the changes of cell numbers and cellular viability after stimulation with menthol. It can be seen from Fig. 4A, menthol (100, 500, 1000 μM) reduced the numbers of synoviocytes after stimulation for 24, 48 and 72 h, respectively. This decrease in synoviocyte proliferation was in a concentration- and time-dependent manner (Fig. 4B). At the mean time, cellular viability was assessed with MTT. As shown in Fig. 4C, menthol at the above three concentrations also reduced cellular viability after stimulation for 48 h, indicating that the reduced cell number was resulted in part from cell death. Further, menthol (500 μM)-induced reduction in cellular viability was evidently reversed by TRPM8 inhibitors CZP (5 μM) (Fig. 4C), indicating the involvement of TRPM8. Similar effects were observed while stimulating the cells with menthol (500 μM) in the presence of intracellular calcium chelator BAPTA-AM (5 μM) or NAD(P)H oxidase inhibitor DPI (5 μM) (Fig. 4C), suggesting an essential role for Ca^{2+} entry-dependent reactive oxygen species generation in this process. In summary, these data indicated that TRPM8/Ca^{2+}/reactive oxygen species signaling was involved in menthol-induced synoviocyte death.

3.5. Apoptosis were involved in menthol-caused synoviocyte death

To test whether menthol induced synoviocyte death associated with apoptosis, we observed the changes of mitochondrial membrane potential and nuclear morphology after stimulation with menthol. It was well known that Rhodamine 123 was used to assess the mitochondrial membrane potential. Menthol (500 μM) induced remarkable mitochondrial membrane depolarization after stimulation for 48 h (Fig. 5A). Simultaneously, the reduction in

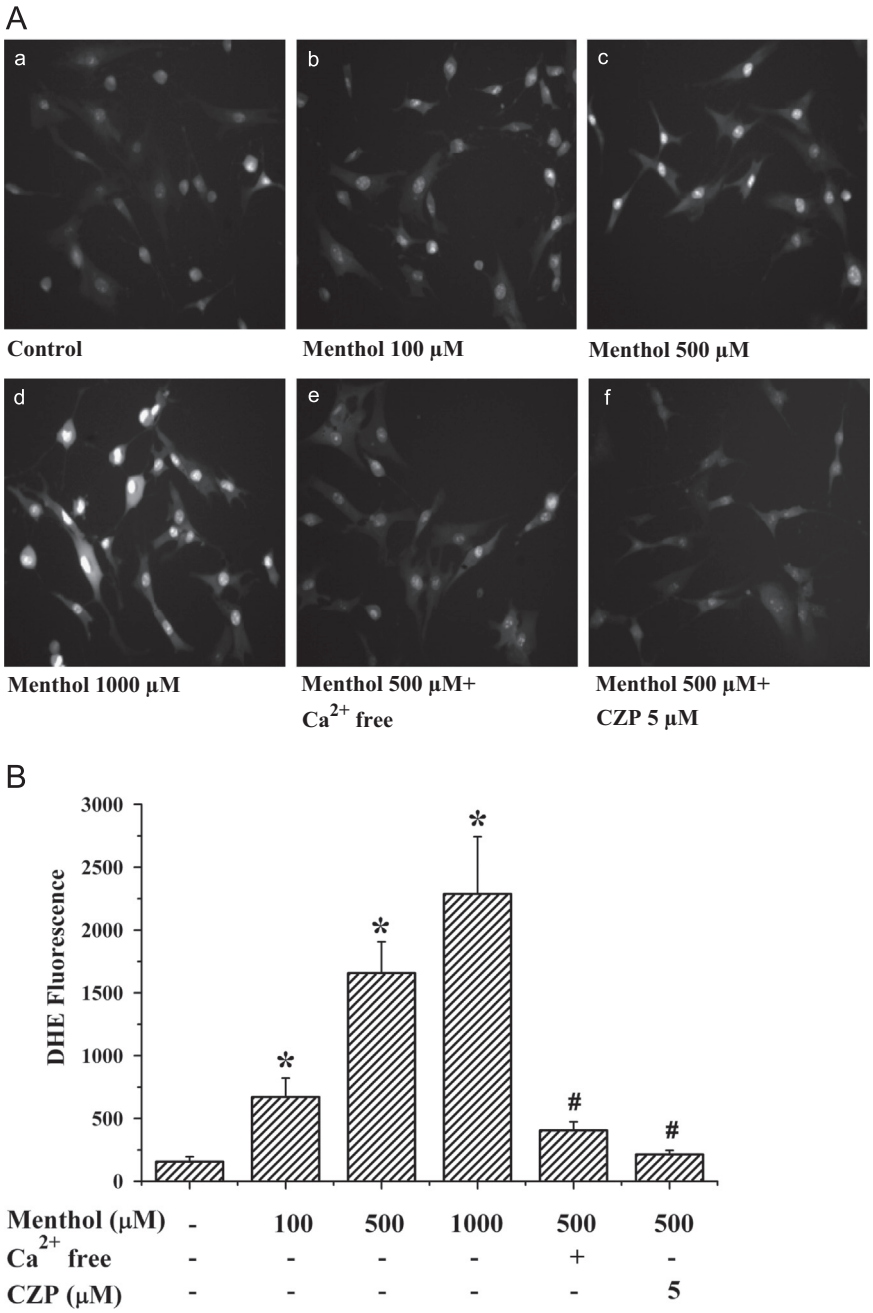

Fig. 3. Menthol induced reactive oxygen species production mediated by TRPM8 activation and calcium entry. (A) Dihydroethidium (DHE) fluorescence images, captured using a 40 × objective, are shown. The fluorescence intensity represents reactive oxygen species concentration. (a) Control cells not treated with either menthol or inhibitors. Cells treated for 1 h with: (b) Menthol (100 μM), (c) Menthol (500 μM), (d) Menthol (1000 μM); (e) Menthol (500 μM) in Ca^{2+} free solution; (f) Menthol (500 μM) after pretreatment with CZP (5 μM). (B) Statistic data of the fluorescence intensity ($n=30$), * showed $P<0.05$, compared with control group; # showed $P<0.05$, compared with menthol (500 μM) group.

mitochondrial membrane potential induced by menthol was significantly reversed by pretreating the cells with CZP (5 μM), BAPTA-AM (5 μM) or DPI (5 μM) (Fig. 5A). These data revealed that mitochondrial membrane depolarization was dependent on calcium entry and reactive oxygen species production mediated by TRPM8 activation. Furthermore, synoviocytes were stained with Hoechst 33342 for detecting apoptotic cells. Menthol (500 μM)-treated cells showed typical apoptotic morphological images of condensed cell nuclei after stimulation for 48 h (Fig. 5B). Similarly, CZP (5 μM), BAPTA-AM (5 μM) or DPI (5 μM), significantly reversed the nuclear condensation induced by menthol (Fig. 5B). In addition, the experiment of caspase 3/7 assay demonstrated that menthol (500 μM) caused synoviocytes apoptosis and evoked an over 3 folds increase in the luminescence of caspase 3/7 compared with the control sample without treatment of menthol (Fig. 5C). The caspase 3/7 activation was also inhibited by pretreatment with CZP (5 μM), BAPTA-AM (5 μM) and DPI (5 μM). These results indicated that menthol induced synoviocyte apoptosis depending on TRPM8 activation-induced calcium entry, reactive oxygen species production and mitochondrial membrane depolarization.

4. Discussion

As a coolant compound, anti-inflammatory applications of menthol had a long history in medicine, whereas the mechanism

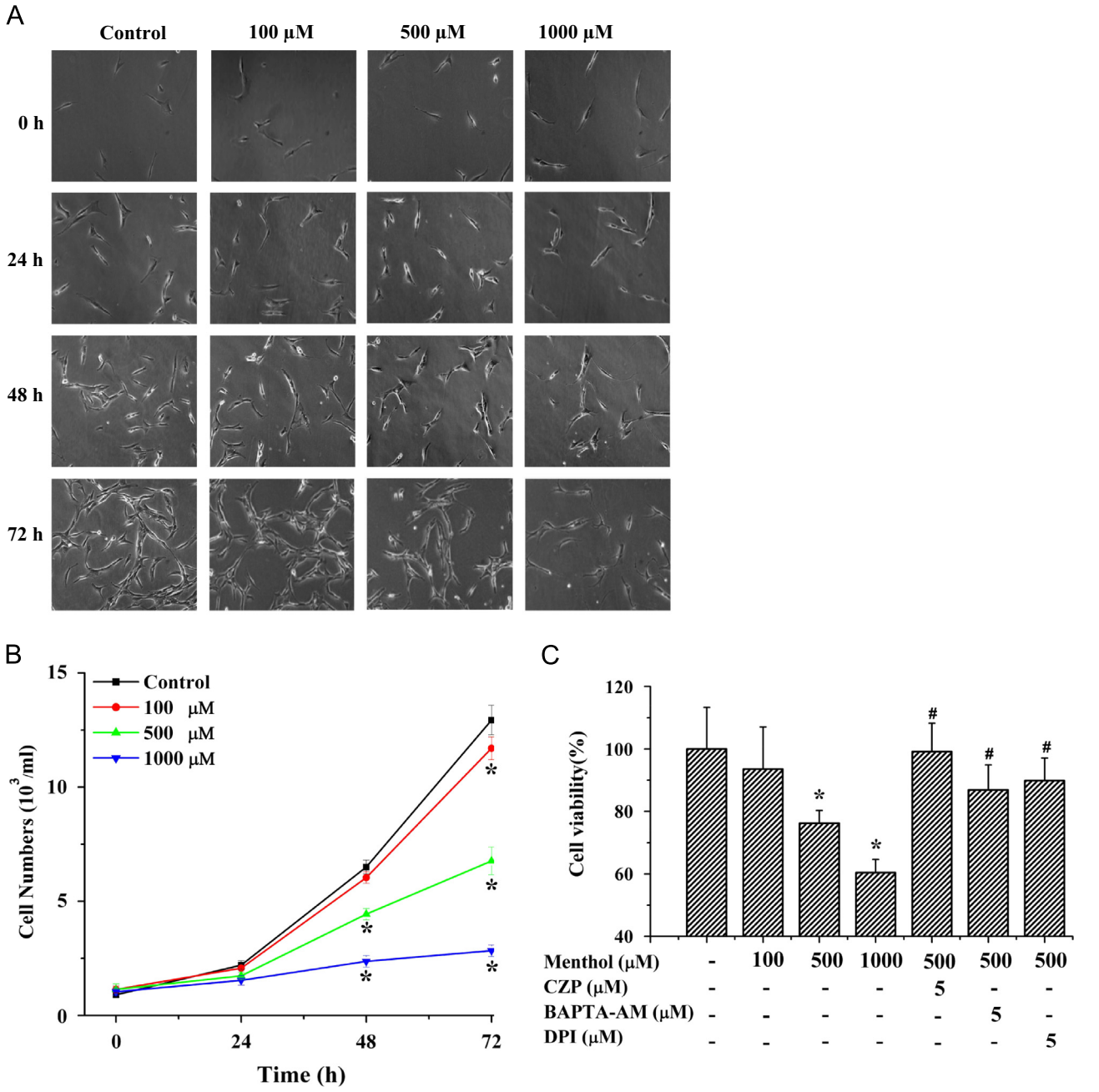

Fig. 4. Menthol decreased the survival of synoviocytes. (A) Synoviocytes were stimulated by menthol (100, 500, 1000 μM) for 24, 48 and 72 h, respectively. (B) Statistic data of cell numbers from experiments shown in A. Each group of cells were grown in triplicate wells and counted three times at different time points ($n=3$). *$P<0.05$, in comparison with control group. (C) Synoviocytes were incubated for 48 h with menthol (100, 500, 1000 μM) and with menthol (500 μM) in the presence of CZP (5 μM), BAPTA-AM (5 μM), DPI (5 μM) ($n=5$). * $P<0.05$, in comparison with control group; # $P<0.05$, in comparison with menthol (500 μM) group.

of these traditional treatments remained obscure. Recently, several temperature sensitive TRP channels, including TRPM8, TRPA1 and TRPV3, have been reported to participate in various inflammatory responses and neuropathic pain sensation (Dhaka et al., 2006; Lumpkin and Caterina, 2007). The activity of these three channels can be either potentiated or attenuated by menthol (Macpherson et al., 2006; Sherkheli et al., 2010). In the present investigation, we demonstrated the expression of TRPM8 channel in synovial fibroblasts from the knee joints of rats with collagen-induced arthritis (Fig. 2) and highlighted the effects of menthol on the proliferation or death of synoviocytes. We found that menthol induced $[Ca^{2+}]_c$ increase, intracellular reactive oxygen species generation, mitochondrial membrane depolarization and eventually led to cell death apoptosis in rat synoviocytes. More importantly, we suggested an essential role for TRPM8 activation in the modulation of these signaling nodes.

The $[Ca^{2+}]_c$ measurement results demonstrated that menthol evoked a rapid and sustained increase in $[Ca^{2+}]_c$ in a dose-dependent manner with an EC_{50} of 250 ± 40 μM (Fig. 1A and B). This $[Ca^{2+}]_c$ increase played key roles in the following signaling steps (experiments in Ca^{2+} free condition or with BAPTA-AM). Removal of extracellular calcium almost eliminated the increase in $[Ca^{2+}]_c$, indicating extracellular Ca^{2+} entry contributed mostly to the $[Ca^{2+}]_c$ increase (Fig. 1C). Furthermore, as putative antagonist of both TRPM8 and TRPV1 (Idris et al., 2010; Karashima et al., 2007; Yudin and Rohacs, 2012), CZP reduced both peak and sustained plateau of $[Ca^{2+}]_c$ (Fig. 1D). Since menthol did not affect the activity of TRPV1 (Macpherson et al., 2006), these results

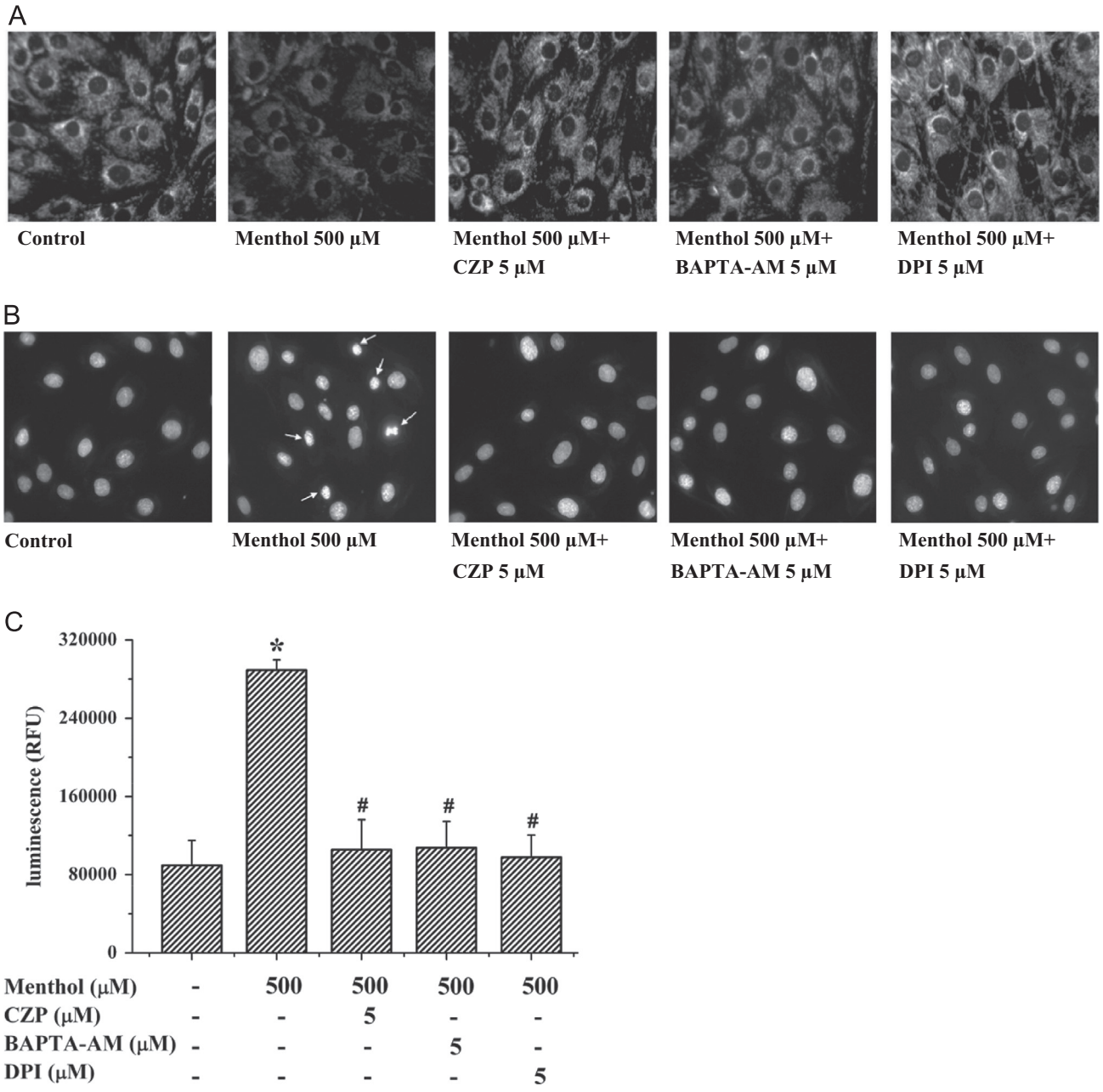

Fig. 5. Menthol induced synoviocyte apoptosis. (A) Synoviocytes were stained with Rhodamine 123 (10 μg/ml) to assess mitochondrial membrane potential. A decrease in fluorescence intensity represented mitochondrial membrane depolarization. The cells were treated for 48 h with menthol (500 μM) alone or in the presence with CZP (5 μM), BAPTA-AM (5 μM) or DPI (5 μM). Control cells were not treated with either menthol or inhibitors. (B) Synoviocytes were stained with Hoechst 33342 (10 μg/ml) to observe the morphology of cell nuclei. (C) The activities of caspase in synoviocytes were measured by Caspase-Glo assay kit to further investigate the lever of cellular apoptosis. $^{*}P<0.05$, compared with control group; $^{\#}P<0.05$, compared with menthol (500 μM) group.

suggested that TRPM8 was most likely responsible for menthol-induced Ca^{2+} entry. In addition, the EC_{50} value for menthol-triggered $[Ca^{2+}]_c$ increase in synoviocytes was close to the reported EC_{50} values of TRPM8 in response to menthol in other cell types such as melanoma cells (286 μM) and *Xenopus* oocytes (196 μM) (Sherkheli et al., 2008; Yamamura et al., 2008), providing collateral evidence for the involvement of TRPM8 in the calcium response. In brief, we can draw a conclusion that the sustained increase of $[Ca^{2+}]_c$ induced by menthol was resulted from TRPM8 activation-conducted extracellular Ca^{2+} entry.

It has been established that intracellular Ca^{2+} overload is a common pathway for cell death by causing mitochondrial Ca^{2+} overload and subsequent mitochondrial disruption. High intracellular Ca^{2+} levels can promote cell death through necrosis, whereas lower Ca^{2+} increases induced by milder insults promote cell death through apoptosis (Shin et al., 2003; Szabadkai and Rizzuto, 2004). Besides, intracellular reactive oxygen species is also considered to be a death signal in apoptosis (Cao et al., 2010). Massive reactive oxygen species production is known to induce prolonged c-Jun NH2-terminal protein kinase activation, Bid phosphorylation, mitochondrial association of BAK/BAX and mitochondrial permeability transition pore opening (Li et al., 2010). Mitochondrial impairment in turn accelerates generation of reactive oxygen species, thereby it results in a positive feedback loop (Zhang and Chen, 2004). Disruption of the mitochondrial membrane potential leads to release of cytochrome c from mitochondria into the cytosol, where cytochrome c triggers caspase-9 activation and initiates caspases cascade which terminates cell to apoptosis (Spierings et al., 2005). Therefore, after the detection of early accumulation of $[Ca^{2+}]_c$ through TRPM8 activation, we

sequentially investigated downstream signals of calcium, including reactive oxygen species production, mitochondrial membrane depolarization, and cell survival. As shown in the present work, menthol elicited marked intracellular reactive oxygen species generation. This reactive oxygen species generation was also inhibited by extracellular Ca^{2+} free condition or CZP pretreatment (Fig. 3), indicating that the reactive oxygen species production induced by menthol was dependent on TRPM8-mediated calcium entry. After that, it was found that menthol depressed the cell proliferation and reduced the cell viability (Fig. 4). Meanwhile, menthol evoked obvious mitochondrial membrane depolarization and typical nuclear condensation, and triggered the caspase-3/7 activation which is a hallmark of apoptosis (Fig. 5). These results suggested that menthol induced apoptosis in synoviocytes, similar to our previous study of capsaicin (Hu et al., 2008). Furthermore, menthol-induced apoptosis was inhibited by pretreatment with TRPM8 antagonist CZP, intracellular calcium chelator BAPTA-AM, or reactive oxygen species inhibitor DPI (Fig. 5). Taken together, our results demonstrated that the synoviocyte apoptosis caused by menthol was resulted from TRPM8-mediated extracellular calcium entry, intracellular reactive oxygen species generation and mitochondrial membrane depolarization.

It may be noted here that, besides TRPM8, menthol can also modulate the responses of TRPV3 and TRPA1 depending on concentration (Macpherson et al., 2006; Sherkheli et al., 2010). As reported, menthol inhibited TRPA1 rather than activated it at concentrations used in the present study (≤ 1 mM) (Macpherson et al., 2006). Furthermore, the estimated EC_{50} for activation of TRPV3 by menthol was as high as 20 mM (Macpherson et al., 2006). The expression of TRPV3 channel was not detected in synoviocytes from RA patients (Kochukov et al., 2006). Although these data partially excluded the contributions of TRPA1 or TRPV3 to menthol-induced synoviocyte death, possible involvement of factors other than TRPM8 could not be completely ruled out and needs further investigation. Moreover, a higher dose (> 1 mM) of menthol may probably evoke pain in human and mouse related to the activation of TRPA1 or TRPV3 channel (Karashima et al., 2007; Brain, 2011; Namer et al., 2005), thus the precise concentration of menthol for clinical products should be considered.

In summary, the present study showed that menthol induced $[Ca^{2+}]_c$ increase, reactive oxygen species generation, mitochondrial membrane depolarization, and eventually resulted in cell death associated with apoptosis in the arthritic rat synovial fibroblasts. This process depended on the activation of TRPM8. Since synoviocyte hyperplasia is critical for RA (Bartok and Firestein, 2010; Neumann et al., 2010), inhibition of synoviocyte hyperplasia is a potentially important target for therapeutic (Cutolo et al., 2007). Our findings in this work could provide some cellular basis for the anti-inflammatory utility of menthol, and may facilitate the development of new therapeutic drugs against RA targeting TRPM8 receptors.

Acknowledgments

This work was supported by the National Natural Science Foundation of China (No. 11204142) and the Fundamental Research Funds for the Central Universities (No. 65010901). Sincere gratitude to *Dr. Kun Song* for his important comments.

References

Al-Bayati, F.A., 2009. Isolation and identification of antimicrobial compound from *Mentha longifolia* L. leaves grown wild in Iraq. Ann. Clin. Microbiol. Antimicrob. 8, 20.

Bartok, B., Firestein, G.S., 2010. Fibroblast-like synoviocytes: key effector cells in rheumatoid arthritis. Immunol. Rev. 233, 233–255.

Biro, T., Toth, B.I., Marincsak, R., Dobrosi, N., Geczy, T., Paus, R., 2007. TRP channels as novel players in the pathogenesis and therapy of itch. Biochim. Biophys. Acta 1772, 1004–1021.

Brain, S.D., 2011. TRPV1 and TRPA1 channels in inflammatory pain: elucidating mechanisms. Ann. NY Acad. Sci. 1245, 36–37.

Cao, X.H., Wang, A.H., Wang, C.L., Mao, D.Z., Lu, M.F., Cui, Y.Q., Jiao, R.Z., 2010. Surfactin induces apoptosis in human breast cancer MCF-7 cells through a ROS/JNK-mediated mitochondrial/caspase pathway. Chem. Biol. Interact. 183, 357–362.

Caspani, O., Zurborg, S., Labuz, D., Heppenstall, P.A., 2009. The contribution of TRPM8 and TRPA1 channels to cold allodynia and neuropathic pain. PLoS One 4, e7383.

Cho, Y., Jang, Y., Yang, Y.D., Lee, C.H., Lee, Y., Oh, U., 2010. TRPM8 mediates cold and menthol allergies associated with mast cell activation. Cell Calcium 48, 202–208.

Clapham, D.E., 2003. TRP channels as cellular sensors. Nature 426, 517–524.

Clapham, D.E., Runnels, L.W., Strubing, C., 2001. The TRP ion channel family. Nat. Rev. Neurosci. 2, 387–396.

Cutolo, M., Straub, R.H., Bijlsma, J.W., 2007. Neuroendocrine-immune interactions in synovitis. Nat. Clin. Pract. Rheumatol. 3, 627–634.

Dhaka, A., Viswanath, V., Patapoutian, A., 2006. Trp ion channels and temperature sensation. Annu. Rev. Neurosci. 29, 135–161.

Eccles, R., 1994. Menthol and related cooling compounds. J. Pharm. Pharmacol. 46, 618–630.

Firestein, G.S., 2003. Evolving concepts of rheumatoid arthritis. Nature 423, 356–361.

Hinoi, E., Ohashi, R., Miyata, S., Kato, Y., Iemata, M., Hojo, H., Takarada, T., Yoneda, Y., 2005. Excitatory amino acid transporters expressed by synovial fibroblasts in rats with collagen-induced arthritis. Biochem. Pharmacol. 70, 1744–1755.

Hu, F., Sun, W.W., Zhao, X.T., Cui, Z.J., Yang, W.X., 2008. TRPV1 mediates cell death in rat synovial fibroblasts through calcium entry-dependent ROS production and mitochondrial depolarization. Biochem. Biophys. Res. Commun. 369, 989–993.

Idris, A.I., Landao-Bassonga, E., Ralston, S.H., 2010. The TRPV1 ion channel antagonist capsazepine inhibits osteoclast and osteoblast differentiation in vitro and ovariectomy induced bone loss in vivo. Bone 46, 1089–1099.

Journigan, V.B., Zaveri, N.T., 2013. TRPM8 ion channel ligands for new therapeutic applications and as probes to study menthol pharmacology. Life Sci. 92, 425–437.

Karashima, Y., Damann, N., Prenen, J., Talavera, K., Segal, A., Voets, T., Nilius, B., 2007. Bimodal action of menthol on the transient receptor potential channel TRPA1. J. Neurosci. 27, 9874–9884.

Kim, S.H., Nam, J.H., Park, E.J., Kim, B.J., Kim, S.J., So, I., Jeon, J.H., 2009. Menthol regulates TRPM8-independent processes in PC-3 prostate cancer cells. Biochim. Biophys. Acta 1792, 33–38.

Kochukov, M.Y., McNearney, T.A., Fu, Y.B., Westlund, K.N., 2006. Thermosensitive TRP ion channels mediate cytosolic calcium response in human synoviocytes. Am. J. Physiol. Cell. Physiol. 291, C424–C432.

Levine, J.D., Alessandri-Haber, N., 2007. TRP channels: targets for the relief of pain. Biochim. Biophys. Acta 1772, 989–1003.

Li, J.Y., Xu, Z.J., Tan, M.Y., Su, W.K., Gong, X.G., 2010. 3-(4-(Benzo[d]thiazol-2-yl)-1-phenyl-1H-pyrazol-3-yl) phenyl acetate induced Hep G2 cell apoptosis through a ROS-mediated pathway. Chem. Biol. Interact. 183, 341–348.

Lumpkin, E.A., Caterina, M.J., 2007. Mechanisms of sensory transduction in the skin. Nature 445, 858–865.

Macpherson, L.J., Hwang, S.W., Miyamoto, T., Dubin, A.E., Patapoutian, A., Story, G.M., 2006. More than cool: promiscuous relationships of menthol and other sensory compounds. Mol. Cell. Neurosci. 32, 335–343.

McInnes, I.B., Schett, G., 2007. Cytokines in the pathogenesis of rheumatoid arthritis. Nat. Rev. Immunol. 7, 429–442.

McKemy, D.D., Neuhausser, W.M., Julius, D., 2002. Identification of a cold receptor reveals a general role for TRP channels in thermosensation. Nature 416, 52–58.

Namer, B., Seifert, F., Handwerker, H.O., Maihofner, C., 2005. TRPAI and TRPM8 activation in humans: effects of cinnamaldehyde and menthol. Neuroreport 16, 955–959.

Neumann, E., Lefevre, S., Zimmermann, B., Gay, S., Muller-Ladner, U., 2010. Rheumatoid arthritis progression mediated by activated synovial fibroblasts. Trends Mol. Med. 16, 458–468.

Park, E.J., Kim, S.H., Kim, B.J., Kim, S.Y., So, I., Jeon, J.H., 2009. Menthol Enhances an Antiproliferative Activity of 1 alpha, 25-Dihydroxyvitamin D-3 in LNCaP Cells. J. Clin. Biochem. Nutr. 44, 125–130.

Patel, T., Ishiuji, Y., Yosipovitch, G., 2007. Menthol: a refreshing look at this ancient compound. J. Am. Acad. Dermatol. 57, 873–878.

Peier, A.M., Moqrich, A., Hergarden, A.C., Reeve, A.J., Andersson, D.A., Story, G.M., Earley, T.J., Dragoni, I., McIntyre, P., Bevan, S., Patapoutian, A., 2002. A TRP channel that senses cold stimuli and menthol. Cell 108, 705–715.

Proudfoot, C.J., Garry, E.M., Cottrell, D.F., Rosie, R., Anderson, H., Robertson, D.C., Fleetwood-Walker, S.M., Mitchell, R., 2006. Analgesia mediated by the TRPM8 cold receptor in chronic neuropathic pain. Curr. Biol. 16, 1591–1605.

Sherkheli, M.A., Gisselmann, G., Vogt-Eisele, A.K., Doerner, J.F., Hatt, H., 2008. Menthol derivative Ws-12 selectively activates transient receptor potential melastatin-8 (Trpm8) ion channels. Pak. J. Pharm. Sci. 21, 370–378.

Sherkheli, M.A., Vogt-Eisele, A.K., Bura, D., Marques, L.R.B., Gisselmann, G., Hatt, H., 2010. Characterization of selective TRPM8 ligands and their Structure Activity Response (SAR) relationship. J. Pharm. Pharm. Sci. 13, 242–253.

Shin, C.Y., Shin, J., Kim, B.M., Wang, M.H., Jang, J.H., Surh, Y.J., Oh, U., 2003. Essential role of mitochondrial permeability transition in vanilloid receptor 1-dependent cell death of sensory neurons. Mol. Cell. Neurosci. 24, 57–68.

Shou, J.Y., Bull, C.M., Li, L., Qian, H.R., Wei, T., Luo, S.A., Perkins, D., Solenberg, P.J., Tan, S.L., Chen, X.Y.C., Roehm, N.W., Wolos, J.A., Onyia, J.E., 2006. Identification of blood biomarkers of rheumatoid arthritis by transcript profiling of peripheral blood mononuclear cells from the rat collagen-induced arthritis model. Arthr. Res. Ther. 8, R28.

Spierings, D., McStay, G., Saleh, M., Bender, C., Chipuk, J., Maurer, U., Green, D.R., 2005. Connected to death: the (unexpurgated) mitochondrial pathway of apoptosis. Science 310, 66–67.

Sun, W.W., Hu, F., Yang, W.X., 2008. Heat and hyposmotic stimulation increase in $[Ca^{2+}]_i$ by Ca^{2+} influx in rat synoviocytes. Chin. Sci. Bull. 53, 548–554.

Szabadkai, G., Rizzuto, R., 2004. Participation of endoplasmic reticulum and mitochondrial calcium handling in apoptosis: more than just neighborhood? FEBS Lett. 567, 111–115.

Thebault, S., Lemonnier, L., Bidaux, G., Flourakis, M., Bavencoffe, A., Gordienko, D., Roudbaraki, M., Delcourt, P., Panchin, Y., Shuba, Y., Skryma, R., Prevarskaya, N., 2005. Novel role of cold/menthol-sensitive transient receptor potential melastatine family member 8 (TRPM8) in the activation of store-operated channels in LNCaP human prostate cancer epithelial cells. J. Biol. Chem. 280, 39423–39435.

Wondergem, R., Bartley, J.W., 2009. Menthol increases human glioblastoma intracellular Ca^{2+}, BK channel activity and cell migration. J. Biomed. Sci. 16, 90.

Yamamura, H., Ugawa, S., Ueda, T., Morita, A., Shimada, S., 2008. TRPM8 activation suppresses cellular viability in human melanoma. Am. J. Cell Physiol. 295, C296–C301.

Yudin, Y., Rohacs, T., 2012. Regulation of TRPM8 channel activity. Mol. Cell. Endocrinol. 353, 68–74.

Zakharian, E., Cao, C., Rohacs, T., 2010. Gating of Transient Receptor Potential Melastatin 8 (TRPM8) channels activated by cold and chemical agonists in planar lipid bilayers. J. Neurosci. 30, 12526–12534.

Zhang, Y., Chen, F., 2004. Reactive oxygen species (ROS), troublemakers between nuclear factor-kappaB (NF-kappaB) and c-Jun NH(2)-terminal kinase (JNK). Cancer Res. 64, 1902–1905.

Zholos, A., 2010. Pharmacology of transient receptor potential melastatin channels in the vasculature. Br. J. Pharmacol. 159, 1559–1571.